

Effective Charge Coupling in Low Dimensional Doped Quantum Antiferromagnets

Suraka Bhattacharjee, Ranjan Chaudhury

Abstract—The interaction between the charge degrees of freedom for itinerant antiferromagnets is investigated in terms of generalized charge stiffness constant corresponding to nearest neighbour t-J model and t_1 - t_2 - t_3 -J model. The low dimensional hole doped antiferromagnets are the well known systems that can be described by the t-J-like models. Accordingly, we have used these models to investigate the fermionic pairing possibilities and the coupling between the itinerant charge degrees of freedom. A detailed comparison between spin and charge couplings highlights that the charge and spin couplings show very similar behaviour in the over-doped region, whereas, they show completely different trends in the lower doping regimes. Moreover, a qualitative equivalence between generalized charge stiffness and effective Coulomb interaction is also established based on the comparisons with other theoretical and experimental results. Thus it is obvious that the enhanced possibility of fermionic pairing is inherent in the reduction of Coulomb repulsion with increase in doping concentration. However, the increased possibility can not give rise to pairing without the presence of any other pair producing mechanism outside the t-J model. Therefore, one can conclude that the t-J-like models themselves solely are not capable of producing conventional momentum-based superconducting pairing on their own.

Keywords—Generalized charge stiffness constant, charge coupling, effective Coulomb interaction, t-J-like models, momentum-space pairing.

I. INTRODUCTION

STRONGLY correlated systems have proved their importance from the time of discovery of antiferromagnetism by Louis Néel [1], [2], [3]. The cuprates are the strongly correlated materials that exhibit many interesting phases upon doping with holes [4], [5], [6]. The phases include the long range ordered antiferromagnetic phase in low doping regime, anomalous non-Fermi liquid-like conducting phase and normal Fermi liquid-like conducting phase at higher doping regions. Interestingly, the optimally doped region shows high temperature superconductivity below the corresponding critical temperature [4], [5], [6]. However, the subsequent discussions about this unconventional superconductivity in cuprates are necessarily accompanied by the possibility of pair formation in these systems. The interaction between the charge degrees of freedom, in effect to the Coulomb potential, are important in determining the

pairing possibility in the strongly correlated doped phases [7]. Study of correlations between the spin and charge degrees of freedom in the itinerant phases of doped cuprates involves the Cu and the O bands [8], [9]. Later, the two band Hamiltonian was reduced to the well known single band t-J model in the low energy limit [10], [11], [12].

The magnetic interaction in 2D systems was studied using many theoretical approaches including Mori's projection technique based on two-time thermodynamic Green's function and Variational Monte Carlo simulations [13], [14], [15], [16], [17]. On the other hand, the 1D t-J model is exactly solvable using Bethe Ansatz at specific values of J/t [18], [19]. Density Matrix Renormalization Group (DMRG) and Transfer Matrix Renormalization Group (TMRG) techniques have been used very successfully in 1D to find the spin correlations away from the super-symmetric points [20], [21]. In 2D too, some attempts using DMRG have been done to find the spin and charge density orders in the doped Hubbard model [22]. In our recent papers, we have developed a non-perturbative quantum mechanical approach to determine the spin correlations in both 2D and 1D doped antiferromagnets, on the basis of generalized spin stiffness constant corresponding to the t-J model [23], [24]. Our results in 1D lead to a very interesting consequence regarding the formation of a new type of spin-spin coupling as doping increases, which is totally distinct from the original antiferromagnetic coupling seen in the insulating and under-doped phases [24]. Our novel prediction was further supported by other experimental and theoretical results [24].

Beside the spin correlations, the attempts to determine the charge correlations include the determination of the inverse dielectric function, involving the standard many body formalism in a Fermi liquid [25]. The total free energy used in the calculation comprises of the Hartree-like term and the exchange correlation contributions. It was found that the Coulomb interaction thus calculated from the inverse of dielectric function, can even change sign and turn attractive if the spin susceptibility is larger than a threshold value [25]. This can trigger the possibility of pairing in some of the doped antiferromagnetic systems. However, the above technique could not determine the charge coupling in strongly correlated phases of the systems, where the double fermionic occupancy on each site is disallowed.

The other approaches include the finding of the local charge stiffness tensor ($D_{\alpha\beta}$) as the response of the system to any change in boundary condition [26]. The component $D_{\alpha\alpha}$ was used to find the optical mass and was shown to be directly proportional to the Drude weight [26]. But the magnitudes of

Suraka Bhattacharjee is with the Department of Condensed Matter Physics and Material Sciences, S.N. Bose National Centre for Basic Sciences, Salt lake, Kolkata, India, (corresponding author, phone: +919874209801, e-mail: surakabhattacha@bose.res.in).

Ranjan Chaudhury is with the Department of Physics, Ramakrishna Mission Vivekananda Educational and Research Institute, Belur, India, (e-mail: ranjan@bose.res.in).

charge stiffness constants, calculated by applying the Lanczos algorithm, were determined only at discrete values of hole concentrations [26], [27]. The Drude weight calculated by exact diagonalization technique in Hubbard cluster shows an increase in the lower doping regime, where the interacting holes are considered as the major carriers [28]. Furthermore, in the over-doped regime, the weakly interacting electrons take the role of the major carriers and the Drude weight falls in magnitude [29]. Moreover, the dynamical conductivity derived based on the memory function technique in terms of the Hubbard operators, was found to be proportional to doping concentration [12]. In order to have a more clearer, definite and detailed understanding of the doping dependences of the charge stiffness, we embark upon an analytical approach.

In this paper, our main aims would be to determine the interaction and coupling between the charge degrees of freedom and to put forward a comparative study between the charge and the spin couplings, determined earlier as functions of doping concentration [23], [24]. Similar to case of spin degrees of freedom, here the doping dependence of charge-charge coupling is studied in terms of the evolution of generalized charge stiffness constant with doping concentration at $T=0$. In the strongly correlated under-doped regime, we have involved the nearest neighbour t-J model preventing the double occupancies. However, in the weakly correlated over-doped regime, we have used the t_1 - t_2 - t_3 -J model with the Gutwiller variational parameter α very small or zero, which allows double occupancies in the system. The results of charge stiffness in the lower doping regions are compared with experimental result on a layered cuprate system and based on the comparison, we have shown a qualitative equivalence between our derived charge stiffness constant and effective Coulomb interaction in the doped regimes [30]. Finally, we have explored the consequences and various possibilities arising from our systematic studies as stated above.

II. RESULTS

A. Calculational Formalism and Numerical Results for Charge Stiffness

1) *Strongly Correlated and with Nearest Neighbour Hopping*: The nearest neighbour t-J model Hamiltonian for strongly correlated electronic systems is [31], [32]:

$$H_{t-J} = H_t + H_J \quad (1)$$

where H_t and H_J represents the hopping and exchange interactions involving nearest neighbour sites, respectively with restrictions on double occupancy at each site. The expression for the kinetic energy Hamiltonian is given as [31], [32]:

$$H_t = \sum_{\langle i,j \rangle, \sigma} t_{ij} X_i^{\sigma 0} X_j^{0\sigma} \quad (2)$$

Here t_{ij} represents the hopping amplitude from j^{th} to i^{th} site and for nearest neighbour $t_{ij}=t$ and the X's are the Hubbard

operators.

Again for the exchange energy part is represented as[31], [32]:

$$H_J = \sum_{\langle ij \rangle} J_{ij} (\vec{S}_i \cdot \vec{S}_j - \frac{1}{4} n_i n_j) \quad (3)$$

where S_i and S_j now represent the localized spin operators corresponding to the i^{th} and j^{th} sites respectively; J_{ij} is the exchange constant involving the i^{th} and the j^{th} site and for nearest neighbour pair $\langle ij \rangle$, $J_{ij}=J$; n_i and n_j are the occupation number operators for the i^{th} and j^{th} site respectively.

As was done earlier for generalized spin stiffness constant (\tilde{D}_s), a similar kind of equation also holds for the generalized charge stiffness (\tilde{D}_c)

$$\tilde{D}_c = \tilde{D}_c^t + \tilde{D}_c^J \quad (4)$$

where \tilde{D}_c^t and \tilde{D}_c^J are the contributions to spin stiffness constant from kinetic energy and exchange energy respectively and are given by [33], [34]:

$$\tilde{D}_c^t = \lim_{\phi \rightarrow 0} \left(\frac{1}{2} \right) \frac{\delta^2 T}{\delta \phi^2} \quad (5)$$

and

$$\tilde{D}_c^J = \lim_{\phi \rightarrow 0} \left(\frac{1}{2} \right) \frac{\delta^2 E_J}{\delta \phi^2} \quad (6)$$

where 'T' and 'E_J' are the kinetic energy expectation value and exchange energy expectation value of the t-J Hamiltonian. ϕ is the magnetic twist corresponding to the Peierl's phase ϕ_σ arising from the presence of the vector potential $A(\vec{r})$ as used in the definition of generalized stiffness constants [33], [34]. The quantity ϕ_σ has the following property for the spin symmetric case:

$$\phi_\downarrow = \phi_\uparrow = \phi \quad (7)$$

[This is unlike the spin asymmetric case, where we had used $\phi_\downarrow = -\phi_\uparrow = \phi$ [23], [24], [34]]

We have evaluated the expectation values in the Gutzwiller state.

$$|\psi_G\rangle = \prod_l (1 - \alpha \hat{n}_{l\uparrow} \hat{n}_{l\downarrow}) |FS\rangle \quad (8)$$

where α is the variational parameter deciding the amplitude for no-double occupancy of any site and $|FS\rangle$ is the Fermi sea ground state [23], [24], [34]. At first we take $\alpha=1$ for completely projecting out the doubly occupied sites.

$$|\psi_G\rangle_{NDOC} = \prod_l (1 - \hat{n}_{l\uparrow} \hat{n}_{l\downarrow}) \prod_{k\sigma} \sum_{ij}^{k_F} C_{i\sigma}^\dagger C_{j-\sigma}^\dagger e^{i(\vec{r}_i - \vec{r}_j) \cdot \vec{k}} |vac\rangle \quad (9)$$

where $|vac\rangle$, i , j and l have the usual meaning [34].

The exchange energy for the spin symmetric case (see (6)) can be written as:

$$E_J = \left(\frac{z t_{eff}^2}{V_{eff}} \right) \frac{NDOC \langle \psi_G | H_J | \psi_G \rangle_{NDOC}}{NDOC \langle \psi_G | \psi_G \rangle_{NDOC}} \quad (10)$$

where 'z' is the co-ordination number i.e., z=4 for 2-D and 2 for 1-D and

$$H_J^I = \vec{S}_i \cdot \vec{S}_j - \frac{1}{4} n_i n_j \quad (11)$$

with ${}_{NDOC} \langle \psi_G | \psi_G \rangle_{NDOC}$ being the normalization factor for the Gutzwiller state $|\psi_G\rangle_{NDOC}$ [24].

Since E_J is ϕ independent [see 10)],

$$\tilde{D}_c^J = 0 \quad (12)$$

Thus $\tilde{D}_c = \tilde{D}_c^t$ always. Hence the exchange energy contribution to charge stiffness vanishes in the entire doping region. This may be completely physical because the interchange of spins has no effect on the carriers in terms of their charge responses.

The total charge stiffness is given by the kinetic energy contribution to charge stiffness (D_c^t) and is derived taking the second order derivative of kinetic energy expectation value in the Gutzwiller state (see (5) and (8)). In 2D,

$$\tilde{D}_c = (-t) \left[\prod_{k_x, \sigma}^{k_F} 4 \cos(k_x a) (1 - \delta)^2 - N_l \prod_{k_x, \sigma}^{k_F} 4 \cos(k_x a) / N^2 \right] \quad (13)$$

(while the vector potential is applied in x-direction) and for 1D,

$$\tilde{D}_c = (-t) \left[\prod_{k, \sigma}^{k_F} 4 \cos(ka) (1 - \delta)^2 - N_l \prod_{k, \sigma}^{k_F} 4 \cos(ka) / N^2 \right] \quad (14)$$

where $N_l = N(1 - \delta)$, N is the total number of sites and 'δ' is the doping concentration and the Fermi momentum k_F in 2-D has the form in the quasi-continuum approximation [23], [24], [34]:

$$k_F = \frac{\sqrt{2\pi(1 - \delta)}}{a} \quad (15)$$

and in 1-D:

$$k_F = (\pi/2a)(1 - \delta) \quad (16)$$

Here it can be noted that the form of \tilde{D}_c^t is similar to that of \tilde{D}_s^t in both one and two dimensions [23], [24], [34]. Hence following the same arguments described in our two previous papers [23], [24], \tilde{D}_c vanishes if at least one value of k_x in 2D (k in 1D) satisfies:

For 2D,

$$k_x a = \pi/2 \quad (17)$$

and for 1D

$$ka = \pi/2 \quad (18)$$

This condition can be satisfied only when $k_F a = \pi/2$. Using the expressions for k_F (see (15,16)), one can get the vanishing conditions are $\delta \rightarrow 1$ and $\delta \leq 0.61$ for 2D model and at $\delta \rightarrow 1$ and $\delta \rightarrow 0$ for 1D [23], [24], [34]. For the vector potential applied in the x-direction, we get the value of $\delta = \delta_c \approx 0.61$, below which the charge stiffness remains zero in 2D.

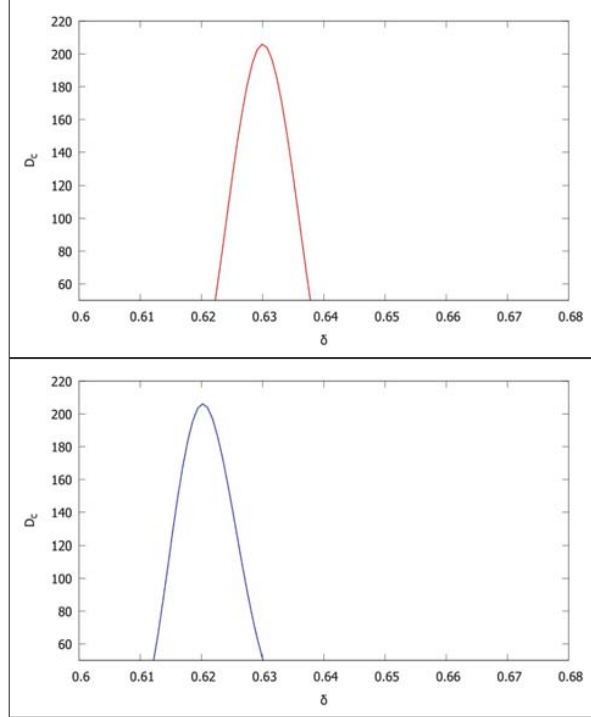


Fig. 1 D_c vs. δ in 2D: (a) lattice size = 700x700; (b) lattice size = 800x800

The total charge stiffness constants derived for the strongly correlated $\alpha=1$ case in 2D and 1D are plotted against δ (see Figs. 1, 2) [23], [24]. In the plots, the total charge stiffness has been scaled down by the number of pairs of mobile holes in the system, to extract an equivalent stiffness corresponding to a pair of mobile charge carriers:

$$D_c = \tilde{D}_c / N_l C_2 \quad (19)$$

In 2D, the scaled charged stiffness constant vanishes upto the critical doping concentration δ_c , followed by a sharp rise in D_c . The charge stiffness again falls drastically with further increase in doping concentration, giving rise to the appearance of a very sharp cusp-like peak in the over-doped region as shown in Figs.1 (a), (b). For the 1D model, D_c shows a maximum in the low doping region, and zero elsewhere (see Figs. 2 (a), (b)). This characteristic behaviour of the coupling between the charge degrees of freedom in the low doping regime is quite physical, since in the under-doped region the correlation is very strong with $\alpha=1$, which prevents two carriers from approaching close to each other and hence the itinerant behaviour of the carriers are largely suppressed. As a result the one charge can not feel the repulsion due to another, giving a zero value to charge stiffness and remains constant throughout the lower doping region. However, the calculation in the over-doped regime is not justified only with the nearest neighbour t-J model. The inclusion of higher neighbour hopping terms are necessary for correctly predicting the behaviour of the higher doping regions.

2) *Weakly Correlated and with Higher Neighbour Hoppings:* In the previous subsection, we have derived

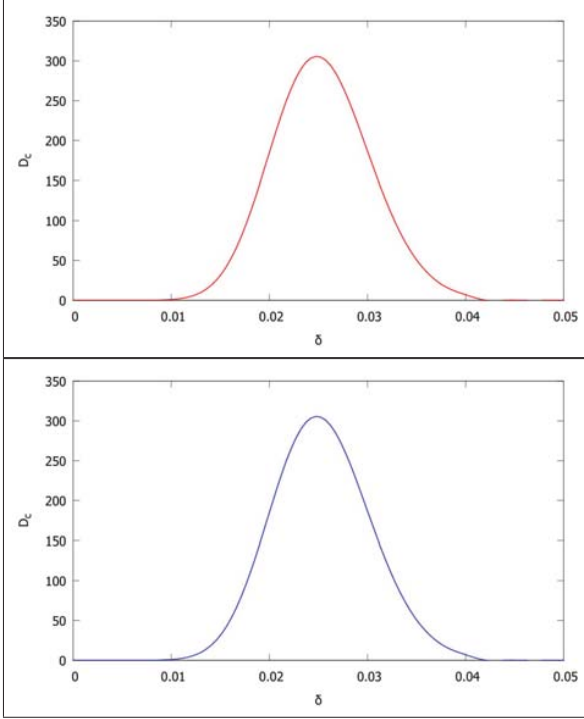


Fig. 2 D_c vs. δ in 1D: (a) lattice length = 1800; (b) lattice length = 1900

the charge stiffness in the strongly correlated regime, considering only the nearest neighbour interaction. Now, in this sub-section we will consider the over-doped regime with very small α and $\alpha=0$ i.e., allowing double occupancies in the system. Moreover, as we have already stated that in the over-doped regime, the higher neighbour hoppings are also significant, so we have incorporated two higher neighbour terms in the t-J model.

The t_1 - t_2 - t_3 -J model is given as [35]:

$$H = -t_1 \sum_{\langle i,j \rangle, \sigma} C_{i\sigma}^\dagger C_{j\sigma} - t_2 \sum_{\langle\langle i,j \rangle\rangle, \sigma} C_{i\sigma}^\dagger C_{j\sigma} - t_3 \sum_{\langle\langle\langle i,j \rangle\rangle\rangle, \sigma} C_{i\sigma}^\dagger C_{j\sigma} + J \sum_{\langle i,j \rangle, \sigma} S_i \cdot S_j \quad (20)$$

where t_1 , t_2 and t_3 represent the first, second and third neighbour hopping amplitudes respectively.

With the vector potential applied along the x-direction as before, we get, in 2D,

$$\tilde{D}_c = - \left[\prod_{k_x, \sigma}^{k_F} 4 \{ (t_1) \cos(k_x a) + (t_2) \cos(2k_x a) + (t_3) \cos(3k_x a) \} (1 - \delta)^2 - \alpha N_l \prod_{k_x, \sigma}^{k_F} 4 \{ (t_1) \cos(k_x a) + (t_2) \cos(2k_x a) + (t_3) \cos(3k_x a) \} / N^2 \right] \quad (21)$$

and in 1D,

$$\tilde{D}_c = - \left[\prod_{k, \sigma}^{k_F} 4 \{ (t_1) \cos(ka) + (t_2) \cos(2ka) + (t_3) \cos(3ka) \} (1 - \delta)^2 - \alpha N_l \prod_{k, \sigma}^{k_F} 4 \{ (t_1) \cos(ka) + (t_2) \cos(2ka) + (t_3) \cos(3ka) \} / N^2 \right] \quad (22)$$

Now, we consider the limiting case with $\alpha=0$ i.e., the double occupancy is totally allowed on the sites and then the Gutzwiller state reduces to that of an ideal Fermi system:

$$|FS\rangle = \prod_{k\sigma}^{k_F} \sum_{ij} C_{i\sigma}^\dagger C_{j-\sigma}^\dagger e^{i(\vec{r}_i - \vec{r}_j) \cdot \vec{k}} |vac\rangle \quad (23)$$

Calculating the kinetic energy in this case ($\alpha=0$) we get for 2D,

$$\tilde{D}_c = - \prod_{k_x, \sigma}^{k_F} 4 \{ (t_1) \cos(k_x a) + (t_2) \cos(2k_x a) + (t_3) \cos(3k_x a) \} (1 - \delta)^2 \quad (24)$$

and for 1D,

$$\tilde{D}_c = - \prod_{k, \sigma}^{k_F} 4 \{ (t_1) \cos(ka) + (t_2) \cos(2ka) + (t_3) \cos(3ka) \} (1 - \delta)^2 \quad (25)$$

From (21)-(25), one can see that the vanishing conditions for \tilde{D}_c corresponding to very small α and $\alpha=0$ in 2D are $\delta \rightarrow 1$ and $\delta \leq \delta_c$, where δ_c depends on the relative magnitudes of t_1 , t_2 and t_3 . For $t_2=t_3=0$ with $\alpha=0$, the value of δ_c becomes 0.61, which is exactly the same as the corresponding value of δ_c obtained for the nearest neighbour t-J model. For 1D t_1 - t_2 - t_3 -J model, D_c vanishes only at $\delta \rightarrow 1$, however, the vanishing conditions for pure t-J model are retained for $t_2=t_3=0$. Thus it can be inferred that the zeros of \tilde{D}_c occur at the same value of doping concentration, when approached from the strongly correlated region or uncorrelated side. The vanishing of charge stiffness in the lower doping regime results from the restrained motion of the charges, as also stated earlier. Here the point where the stiffness exhibits a jump (δ_c) appears in the optimal doping region which is much lower than that was obtained from the nearest neighbour t-J model (i.e., $\delta=0.61$). The charge stiffness again falls with further increase in doping concentration, due to the the presence of large number of vacancies in the system. Hence, this δ_c may very well represent a point of possible quantum phase transition between two regions of constant stiffness separated by a sharp peak. The recent experimental observations from some of the doped correlated systems seem to have a link with this result of ours [36].

The plots of D_c for weakly correlated t_1 - t_2 - t_3 -J model in two dimension, are presented in Fig. 3. The corresponding plots for 1D are given in Fig. 4. The values of t_2/t_1 and t_3/t_1 were determined by fitting the tight binding Fermi surfaces to the experimental results on $\text{La}_{2-x}\text{Sr}_x\text{CuO}_4$ and Bi_{2212} [37], [38].

The second neighbour hopping amplitude was found to be of opposite sign with respect to the first neighbour hopping. Here, we have done the calculations for a range of feasible values of t_2 and t_3 and presented a result for a few sets of t_2/t_1 and t_3/t_1 .

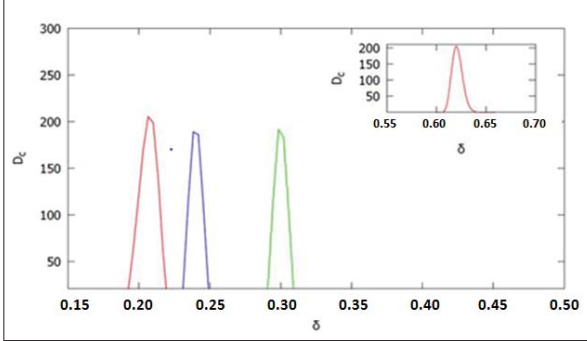


Fig. 3 D_c vs. δ for 2D t_1 - t_2 - t_3 -J model, with $\alpha=0$; (a) peak at $\delta \sim 0.29$ ($t_2=-0.53t_1, t_3=0.24t_1$) [green line]; (b) peak at $\delta \sim 0.23$ ($t_2=-0.52t_1, t_3=0.45t_1$) [blue line]; (c) peak at $\delta \sim 0.19$ ($t_2=-0.6t_1, t_3=0.56t_1$) [red line] [in the inset is shown D_c vs. δ for $t_2=t_3=0$; the peak is seen at $\delta \sim 0.61$]

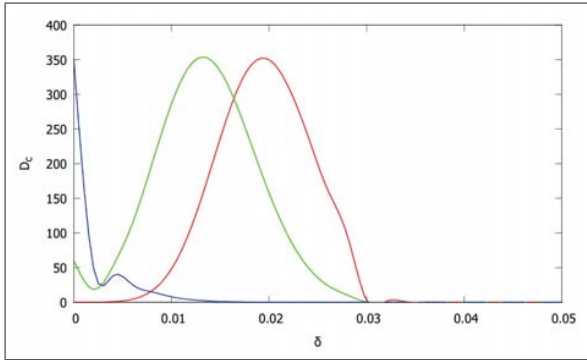


Fig. 4 D_c vs. δ for 1D t_1 - t_2 - t_3 -J model, with $\alpha=0$; (a) peak at $\delta \sim 0.02$ ($t_2=-0.01t_1, t_3=0.005t_1$) [red line]; (b) peak at $\delta \sim 0.013$ ($t_2=-0.02t_1, t_3=0.01t_1$) [green line]; (c) peak at $\delta \rightarrow 0$ limit ($t_2=-0.04t_1, t_3=0.02t_1$) [blue line]

Fig. 3 shows that the maximum in D_c shifts to the optimal doping region for range of values of t_2/t_1 and t_3/t_1 . Again, the peak gradually shifts to further lower doping concentration for relatively higher magnitudes of second and third neighbour hopping amplitudes ($|t_2|$ and $|t_3|$) (see Fig. 3). Similarly, in 1D too, the peak in D_c shifts to very low doping regime as $|t_2|$ and $|t_3|$ are enhanced and the position of the peak reaches $\delta \rightarrow 0$ limit at $t_2 \approx -0.04t_1$ and $t_3 \approx 0.02t_1$ (see (Fig. 4).

B. Comparison with Experimental Results

In the present sub-section, we would to try compare our results of charge stiffness with effective Coulomb interaction and prove our conjecture already put forward in the 'Introduction' part. In this context, it must be pointed out that no direct experimental results are available for effective Coulomb interaction (V_{eff}^{exp}) of layered cuprate systems. So,

one can extract V_{eff}^{exp} from results of optical experiments, using the constitutive equations as given below. V_{eff} in the long wavelength limit of the staggered magnetization is related to the imaginary conductivity by the standard constitutive equations in the continuum limit [39]:

$$\epsilon'(\omega) = 1 - \frac{4\pi\sigma''}{\omega} \quad (26)$$

$$V_{eff}(\omega) = \frac{V_0}{\epsilon'(\omega)} \quad (27)$$

leading to

$$V_{eff}^{exp}(\omega) = \frac{V_0}{1 - \frac{4\pi\sigma_{exp}''}{\omega}} \quad (28)$$

with V_0 being the bare Coulomb interaction, ϵ'_{exp} the real part of the dynamic dielectric function and σ''_{exp} representing the imaginary part of the dynamic conductivity, extracted experimentally.

The most of the experiments carried out on the planes of lightly and optimally doped $\text{La}_{2-x}\text{Sr}_x\text{CuO}_4$ are at high frequency and at much higher temperatures ($>>0\text{K}$), which are not suitable for comparison with our results. However, here, we have considered a transmitted THz time-domain spectroscopy (THz-TDS) on $\text{La}_{2-x}\text{Sr}_x\text{CuO}_4$ [30]. The effective Coulomb interaction is derived from the experimentally extracted imaginary conductivity using (28). We have found that the effective Coulomb interaction is small and remains almost constant throughout the lower doping region (in the calculation, we have used the bare onsite Coulomb interaction $V_0=3.5\text{eV}$ in the undoped phase [30]). This result is similar to that of our derived charge stiffness constant as a function of doping in the under-doped region. Further, we are awaiting more experimental results in the low frequency region and our theoretical prediction for effective Coulomb repulsion to be directly tested by experiments in near future

III. DISCUSSION

The generalized charge stiffness constants for 2D and 1D t-J-like models in strong and weak correlation limits are calculated. A weak dimensional dependence is seen for coupling between the mobile charge degrees of freedom. Furthermore, our calculations bring out several important features and conclusions covering various aspects of correlated fermionic systems in low dimensions.

The D_c in 2D remains zero upto $\delta=\delta_c=0.61$ and then exhibits a sharp rise in value. δ_c shifts to optimal doping region when t_2 and t_3 are included. The available experimental results also show a similar behaviour in lower doping region [30]. Thus a qualitative equivalence of charge stiffness constant and effective Coulomb interaction is established in the low δ regime. Moreover, as δ is increased the localized insulating behaviour of the holes are lost and the charges become itinerant above the strongly correlated under-doped region. Keeping this in mind, one can take the continuum approximation and observe a point of discontinuity in the Lindhard function at $q=2k_F$ ('q' is the charge ordering wave vector). Now, using different values of the ordering wave

vector 'q', it can be shown that the discontinuity appears at some in the optimal doping region, Fermi momentum being related to δ by (15) [40], [41]. This discontinuity in the Lindard function also manifests itself in the calculation of dielectric function and as a result V_{eff} shows a jump at the corresponding value of δ [40], [41], [42] (the details of the calculation might be published somewhere else). This characteristic behaviour is very similar to our result of derived charge stiffness constant (see Fig. 1), which possibly signifies the tendency of the formation of charge ordering or charge density waves as the idea put forward by Overhauser [43]. Hence, the similarity in the behaviour of our derived charge stiffness constant and effective Coulomb interaction proves the qualitative equivalence between the two even in the over-doped regime of these doped itinerant systems. Considering the equivalence, we have drawn a phase diagram of the doped antiferromagnets in 2D, based on their charge responses from the t_1 - t_2 - t_3 -J model (see Fig. 5). We have shown the values of critical doping concentration (δ_c) for different values of t_3/t_1 ratio, taking t_2/t_1 as parameter. From Fig. 5, one can also notice that for a particular value of t_3/t_1 , the transition between the two regions of different charge couplings, takes place at a lower value of doping concentration for higher values of $|t_2/t_1|$.

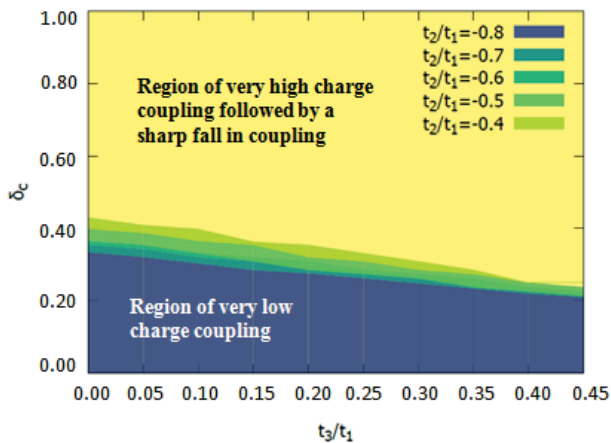


Fig. 5 Phase diagram showing the critical doping concentration (δ_c), separating the regions of charge couplings, as a function of t_3/t_1 (with t_2/t_1 ratio as the parameter). The regions of doping concentration below δ_c represent the regime very low charge coupling and above δ_c , the interaction shows a very high value, followed by a sharp fall. The different colours are used for different ratios of t_2/t_1 [$\alpha=1$ has been taken]

Interestingly, the spin stiffness constant (D_s) for 2D t-J model also shows a point of inflection (indicative of a possible phase transition) at the same δ , where D_c exhibits the sharp rise [23]. Furthermore, D_c and D_s show almost identical behaviour for $\delta > \delta_c$, i.e. in the over-doped regime, which is an expected behaviour of Fermi liquid-like phases. In the under-doped regime however, the behaviour of the two stiffness constants are very different. Thus it can be concluded that the lower doping region represents an anomalous conducting phase, whereas the over-doped regime is normal Fermi liquid-like metallic in nature.

The results for 1D t-J model is also quite important. The quantity D_c in 1D vanishes at $\delta=0$ and $\delta \rightarrow 0$ and exhibits a maximum in the lower doping region. The peak shifts to further lower doping as the higher neighbour hopping amplitudes are increased and reaches the $\delta \rightarrow 0$ limit at critical values of t_2 and t_3 (see Figs. 2, 4). In a recent paper, we have shown that in one dimension, D_s displays a high value at $\delta \rightarrow 0$ limit and falls rapidly with increase in doping concentration [24]. The drastic fall is immediately followed by the formation of a peak in the under-doped regime [24]. Hence, we see that D_s and D_c show completely distinct behaviour only in the very low doping region, whereas they show a similar trend as doping is slightly increased.

One more point that may be highlighted is that, in our calculation we do not get any region of negative charge stiffness, as is expected from the stability criteria (see (5), (6)). Therefore, the effective interaction between the mobile charge degrees of freedom never becomes attractive in these models and the reduction in magnitude of charge stiffness results in the decrease in effective Coulomb repulsion only. This reduction in effective Coulomb repulsion with increase in hole doping in turn gives rise to the enhanced possibility of fermionic pair formation in doped magnetic systems in 2D, provided some other attractive pairing mechanism is present. Thus we have established that the t-J-like models, on their own, can not produce Cooper pairing in q-space. However, in some of the recent works, real space pairing has been studied in the framework of the t-J-like models mostly in the under-doped phase [44], [45], [46]. Hence, our detailed calculations and results throw serious doubt on the feasibility of the momentum-space pairing based only on the t-J-like models as was advocated earlier [47], [48], [49].

REFERENCES

- [1] M.L. Néel, Ann.Phys. 11, 232 (1936)
- [2] N.F.Mott, "Metal-Insulator Transition", Taylor and Francis, London, Second edition (1990)
- [3] J.Hubbard, Proc.R.Soc.London A 276, 238 (1963)
- [4] D.Rybicki, M.Jurkutat, S.Reichardt, C.Kapusta, J.Haase, Nature Communications 7, 11413 (2016)
- [5] D.Chakraborty, C.Morice, C.Pépin, Phys.Rev.B 97, 214501 (2018)
- [6] K.V.Mitsen, O.M.Ivanenko, Physics-Uspekhi 60, 402 (2017)
- [7] M.Vojta, S.Sachdev, Phys.Rev.Lett. 83, 3916 (1999)
- [8] A.Aharony, R.J.Birgeneau, A.Coniglio, M.A.Kastner, H.E.Stanley Phys.Rev.Lett. 60, 1330 (1988)
- [9] R.J.Birgeneau, M.A.Kastner, A.Aharony, Z.Phys. B: Cond. Mat. 71, 57 (1998)
- [10] F.C.Zhang, T.M.Rice, Phys.Rev.B 41, 7243 (1990)
- [11] N.M.Plakida, R.Hayn, J.L.Richard, Phys.Rev.B 51, 16599 (1995)
- [12] N.M.Plakida, Z.Phys.B 103, 383 (1997)
- [13] G. Jackeli, N.M.Plakida, Theor.Math.Phys.114, 335 (1998)
- [14] A.A.Vladimirov, D.Ihle, N.M.Plakida, Phys.Rev.B 80, 104425 (2009)
- [15] A.A.Vladimirov, D.Ihle, N.M.Plakida, Phys.Rev.B 83, 024411 (2011)
- [16] J.Kaczmarczyk, J.Spalek, T.Schickling, J.Bünemann, Phys.Rev.B 88, 115127 (2013)
- [17] D.J.Scalapino, "Handbook of High-Temperature Superconductivity", edited by J.R.Schrieffer, J.S.Brooks, Chapter-XIII, Springer, NewYork (2007)
- [18] H.C.Jiang, T.P.Devereaux, Science 365, 1424 (2019)
- [19] M.Ogata, M.U.Luchini, S.Sorella, F.F.Assaad, Phys.Rev.Lett. 66, 2388 (1991)
- [20] N.Kawakami, S.K. Yang, Phys.Rev.Lett. 65, 2309 (1990)
- [21] B.Sciolla, A.Tokuno, S.Uchino, P.Barmettler, T.Giamarchi, C.Kollath, Phys.Rev.A 88, 063629 (2013)
- [22] J.Sirker, A.Klümper, Phys.Rev.B 66, 245102 (2002)

- [23] S.Bhattacharjee, R.Chaudhury, *Physica B* 500, 133 (2016)
- [24] S.Bhattacharjee, R.Chaudhury, *J.Low Temp.Phys.* 193, 21 (2018)
- [25] R.Chaudhury, S.S.Jha, *Pramana* 22, 431 (1984); Y.A.Uspenskii, *Sov.Phys. JETP* 49, 822 (1979); V.L.Ginzburg, D.A.Kirzhnits, *Phy.Rep.* C4, 344 (1972)
- [26] D.Poilblanc, *Phy.Rev.B* 44, 9562 (1991)
- [27] J.Jaklič, P.Prelovšek, *Phy. Rev. B* 52, 6903 (1995)
- [28] E.Blackburn, J.Chang, M.Hücker, A.T.Holmes, N.B.Christensen, R.Liang, D.A.Bonn, W.N.Hardy, U.Rütt, O.Gutowski, M.V.Zimmermann, E.M.Forgan, S.M.Hayden, *Phy.Rev.Lett.* 110, 137004 (2013)
- [29] E.Dagotto, A.Moreo, F.Ortolani, D.Poilblanc, J.Riera, *Phy.Rev.B* 45, 10741 (1992)
- [30] D.Nakamura, Y.Imai, A.Maeda, I.Tsukada, *J.Phys.Soc.Jpn.* 81, 044709 (2012)
- [31] R.Chaudhury, *Theor.Math.Phys.* 136, 1022 (2003)
- [32] D.Volhardt, *Rev.Mod.Phys.* 56, 99 (1984); F.C.Zhang, T.M.Rice, *Phys.Rev. B* 37, 3759 (1988)
- [33] W.Kohn, *Phys.Rev. A* 133, 171 (1964); D.J.Thouless, *Phys.Rep.* 13, 94 (1074); B.S.Shastry, B.Sutherland, *Phys.Rev.Lett.* 65, 243 (1990); P.A.Bares, G.Blatter, *Phys.Rev.Lett.* 64, 2567 (1990)
- [34] R.Chaudhury, *J.Phys.:Condens.Matter* 19, 496203 (2007)
- [35] V.N.Kotov, O.P.Sushkov, *Phy.Rev. B* 70, 195105 (2004)
- [36] J.Leshen, M.Kawai, I.Giannakis, Y.Kaneko, Y.Tokura, S.Mukherjee, W.C.Lee, P.Ayanjian, *Communication Physics* 2, 36 (2019)
- [37] T.Tohyama, S.Nagai, Y.Shibata, S.Maekawa, *J.Low Temp. Phys.* 117, 211 (1999)
- [38] T.Tohyama, S.Nagai, Y.Shibata, S.Maekawa, *Phys.Rev.B* 82, 4910 (1999)
- [39] N.W.Ashcroft, N.D.Mermin, "Solid State Physics", chapter-XVII, Harcourt College Publishers (1976), Preprint (2015)
- [40] V.L.Ginzburg, D.A.Kirzhnits, "High-Temperature Superconductivity", by chapter-III, New York: Consultants Bureau (1982)
- [41] G.F.Giuliani, G.Vignale, "Quantum Theory of the Electron liquid", chapter-IV,V, Cambridge University Press (2005)
- [42] The inverse of the effective Coulomb interaction is proportional to the modulus of the free particle Lindhard function and the Lindhard function exhibits a discontinuity at $q=2k_F$
- [43] A.W.Overhauser, *Phy.Rev.* 128, 1437 (1962)
- [44] M.Zegrodnik, J.Spalek, *Phy.Rev.B* 98, 155144 (2018)
- [45] J.Spalek, M.Zegrodnik, J.Kaczmarczyk, *Phy.Rev.B* 95, 024506 (2017)
- [46] J.Spalek, *Cond.Mat.Phys.* 11, 455-462 (2008)
- [47] V.Yu.Yushankhai, N.M.Plakida, P.Kalinay, *Physica C* 174, 401 (1991)
- [48] Kazuhiko Sakakibara, Ikuo Ichinose, Tetsuo Matsui, *Phys.Rev.B* 46, 14779 (1992)
- [49] N.M.Plakida, V.S. Oudovenko, P.Horsch, and A.I.Liechtenstein, *Phy.Rev.B* 55, R11997(R) (1997)